

Moving Horizon \mathcal{H}_∞ Tracking Control of Wheeled Mobile Robots With Actuator Saturation

Hong Chen, *Member, IEEE*, Miao-Miao Ma, Hu Wang, Zhi-Yuan Liu, and Zi-Xing Cai

Abstract—This brief considers the dynamic tracking control of wheeled mobile robots (WMR), in the presence of both actuator saturations and external disturbances. A computationally tractable moving horizon \mathcal{H}_∞ tracking scheme is presented, where a constrained \mathcal{H}_∞ control problem is solved at each sampling time with the update of not only the initial condition but also the prediction model. Closed-loop tracking properties inclusive of \mathcal{L}_2 disturbance attenuation are discussed in the framework of dissipation theory. Simulation results are given.

Index Terms—Control constraints, disturbance attenuation, \mathcal{H}_∞ tracking, moving horizon control, wheeled mobile robot (WMR).

I. INTRODUCTION

WHEELED mobile robots (WMR) are more and more widely used in every aspect of the society. In many cases, such as in industry or in military affairs, we need to make the robot move along a specified trajectory, and actually, this task can be theoretically described as a control problem consisting of planning and tracking a trajectory in the presence of disturbances and uncertainties. For tracking problem, various control methods have been suggested, based on nonlinear feedback inclusive of backstepping technique and sliding mode (e.g., [1]–[5]), and dynamic feedback linearization (e.g., [6] and [7]).

Recently, there is a growing interest in the control problem of nonholonomic systems with input constraints, for any actuator suffers saturation. Based on the kinematic and simplified dynamic model of a WMR, [8] develops a model-based control design for the stabilization and tracking problem with input constraints, by the use of passivity and normalization. In [9] and [10], the kinematic tracking problem in the presence of velocity constraints is discussed, using the backstepping technique and the Lasalle's invariance principle. With the rapid development of computing, moving horizon control, mostly referred to as model predictive control (MPC), has become an attractive feed-

back strategy for controlling WMRs due to its advantages of explicitly handling time-domain constraints and nonlinear dynamics [11]–[13], and also due to its discontinuous property that enables to design controllers with simultaneous tracking and regulation capability [14]. But none of these take external disturbances into consideration, which inevitably affect the tracking performance. For the disturbance attenuation problem of a controlled WMR, a few approaches have been proposed. For example, [15] presents an adaptive robust motion controller to deal with system uncertainties and disturbances; and [16] exploits a Kalman-based active observer controller for the path following of WMRs subject to external disturbances, modeling errors and noise.

As mentioned before, there are many works considering control constraints or disturbance attenuation, but few deal with both of them simultaneously. One of the difficulties is that in order to achieve good performance, we usually need large control actions (or high-gain controllers), which easily leads to constraint violations. With the online solution of the optimization problem, MPC presents a possibility of managing online the tradeoff between disturbance attenuation and control constraints. In [17], we present a robust MPC scheme with performance adaptation for linear systems with control and output constraints. A constrained \mathcal{H}_∞ control problem is solved in moving horizon fashion and the \mathcal{H}_∞ norm from disturbances to controlled outputs is online minimized, whereas classic MPC schemes minimize quadratic cost functionals and do not consider disturbances explicitly. In this brief, we extend the work in [17] and provide a solution to the WMR tracking control problem in the *simultaneous* presence of control constraints and external disturbances. An \mathcal{H}_∞ tracking performance for disturbance attenuation is achieved although there are actuator saturations.

This brief is organized as follows. Section II describes the control problem to be studied. Section III presents the moving horizon \mathcal{H}_∞ tracking scheme and the computationally tractable algorithm. Closed-loop tracking properties are discussed, too. Section IV gives the simulation results.

II. PROBLEM STATEMENT

The wheeled mobile robot studied in this brief is a two-wheel differentially driven vehicle with a passive caster in the front (see Fig. 1), and its dynamic model can be given by

$$\begin{cases} \dot{x} = v \cos \phi \\ \dot{y} = v \sin \phi \\ \dot{\phi} = \omega \\ \dot{v} = \beta_1(\tau_1 + \tau_2) + \beta_3 w_1 \\ \dot{\omega} = \beta_2(\tau_1 - \tau_2) + \beta_4 w_2 \end{cases} \quad (1)$$

where (x, y) are the position coordinates and ϕ is the angle between the heading direction and the x -axis; (v, ω) are, re-

Manuscript received July 23, 2007; revised January 11, 2008. Manuscript received in final form January 11, 2008. Current version published February 25, 2009. Recommended by Associate Editor L. Villani. This work was supported in part by the National Science Fund of China for Distinguished Young Scholars under Contract 60725311 and by the Program for New Century Excellent Talents in University.

H. Chen, M.-M. Ma, and H. Wang are with the Department of Control Science and Engineering, Jilin University, 130025 Changchun, PR China (e-mail: chenhh@jlu.edu.cn; mamiomiao@email.jlu.edu.cn; wanghu63@yahoo.com.cn).

Z.-Y. Liu is with the Department of Control Science and Engineering, Harbin Institute of Technology, 150001 Harbin, PR China (e-mail: liuzhi_hit@hit.edu.cn).

Z.-X. Cai is with the College of Information Science and Engineering, Central South University, 410083 Changsha, PR China (e-mail: zxcail@mail.csu.edu.cn).

Digital Object Identifier 10.1109/TCST.2008.2000985

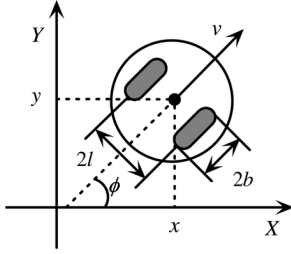


Fig. 1. WMR.

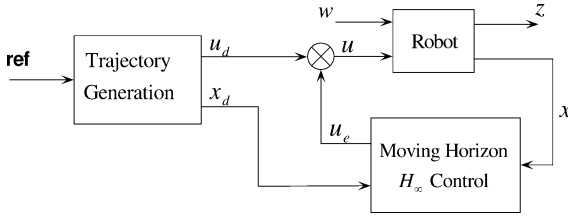


Fig. 2. Two DOF controller design.

spectively, the linear velocity and the angular velocity of the robot; (τ_1, τ_2) are the drive torques provided by two motors attached to the rear wheels, which are considered as control inputs; (w_1, w_2) are two collective disturbances representing external (or unmodeled) forces and torques in the directions of the linear and angular velocities. In model (1), we neglect the ground friction, the centrifugal and Coriolis forces and the inertia of the wheels. Indeed, some of these can be considered in the form of disturbances. Moreover, $\beta_1 = 1/(bm)$, $\beta_2 = l/(bI)$, $\beta_3 = 1/m$, $\beta_4 = 1/I$, where m and I are the mass and the moment of inertia of the WMR, respectively; $2l$ is the length of the rear wheel axis and b is the radius of the wheels. We stress that some uncertainties such as parametric uncertainties in β_1 and β_2 can also be considered in this setup as additive disturbances. It is known that WMR is a typical nonholonomic system with the nonholonomic constraint $\dot{x} \sin \phi - \dot{y} \cos \phi = 0$, which specifies the non-slip of the wheel in the lateral direction. Moreover, due to actuator saturation, the control inputs are constrained as

$$|\tau_j(t)| \leq \tau_{j,\max} \quad \forall t \geq t_0, \quad j = 1, 2. \quad (2)$$

We consider in this brief the tracking control problem of WMRs in the presence of both control constraints and disturbances, and want to achieve a possible smallest \mathcal{L}_2 gain from the disturbance to the tracking error while satisfying control constraints. To this end, we adapt the two degree-of-freedom (DOF) controller design (e.g., [18]), as shown in Fig. 2. The trajectory generation block is to synthesize feasible nominal trajectories (including state x_d and input u_d), where the differential flatness technique is applied. This will be sketched in Section IV. The moving horizon \mathcal{H}_∞ control block is used to correct the tracking error caused by disturbances and uncertainties. This is the main topic of the brief and will be detailed in the following.

III. MOVING HORIZON \mathcal{H}_∞ TRACKING: AN LMI APPROACH

In this section, we first propose a moving horizon control scheme for the previous tracking problem, then discuss the closed-loop properties of the tracking error system including \mathcal{L}_2 disturbance attenuation and the satisfaction of control constraints. Finally, we give a computationally tractable algorithm.

A. Control Scheme

For generality, we consider the following nonlinear system described by:

$$\begin{aligned} \dot{x}(t) &= f(x(t), u(t), w(t)) \\ x(t_0) &= x_0, t \geq t_0 \end{aligned} \quad (3a)$$

$$z(t) = h(x(t), u(t), w(t)) \quad (3b)$$

with control constraints

$$|u_j(t)| \leq u_{j,\max}, \quad j = 1, 2, \dots, m_2, \quad t \geq t_0 \quad (4)$$

where $x \in \mathbb{R}^n$ denotes the state, $w \in \mathbb{R}^{m_1}$ is the external disturbance, $u \in \mathbb{R}^{m_2}$ is the control input, and $z \in \mathbb{R}^{p_1}$ is the performance output. We assume furthermore that the vector fields $f : \mathbb{R}^n \times \mathbb{R}^{m_1} \times \mathbb{R}^{m_2} \rightarrow \mathbb{R}^n$ and $h : \mathbb{R}^n \times \mathbb{R}^{m_1} \times \mathbb{R}^{m_2} \rightarrow \mathbb{R}^{p_1}$ are sufficiently smooth.

Let (x_d, u_d, z_d) be the reference trajectory, which is in general time-varying and satisfies the unperturbed nonlinear system, i.e.,

$$\begin{aligned} \dot{x}_d(t) &= f(x_d(t), u_d(t), 0) \\ x_d(t_0) &= x_{d0}, \quad t \geq t_0 \end{aligned} \quad (5a)$$

$$z_d(t) = h(x_d(t), u_d(t), 0). \quad (5b)$$

Moreover, $u_d(\cdot)$ has to respect the control constraint (4) to ensure the constrained tracking control problem reasonable. By defining the error vectors

$$x_e := x - x_d, \quad u_e := u - u_d, \quad z_e := z - z_d \quad (6)$$

we linearize (3) about the reference to approximate the error dynamics starting from $(t_0, x_e(t_0))$ as

$$\dot{x}_e(t) = A(t)x_e(t) + B_1(t)w(t) + B_2(t)u_e(t) \quad (7a)$$

$$z_e(t) = C(t)x_e(t) + D_1(t)w(t) + D_2(t)u_e(t) \quad (7b)$$

with the matrices

$$\begin{pmatrix} A(t) & B_1(t) & B_2(t) \\ C(t) & D_1(t) & D_2(t) \end{pmatrix} := \begin{pmatrix} \frac{\partial f}{\partial x} & \frac{\partial f}{\partial w} & \frac{\partial f}{\partial u} \\ \frac{\partial h}{\partial x} & \frac{\partial h}{\partial w} & \frac{\partial h}{\partial u} \end{pmatrix} \bigg|_{(x_d(t), u_d(t), 0)}. \quad (8)$$

The control inputs in the error system (7) are then constrained by

$$|u_{e,j}(t)| \leq u_{j,\max} - |u_{d,j}(t)| \quad \forall t \geq t_0, \quad j = 1, 2, \dots, m_2. \quad (9)$$

The basis of model predictive control is the prediction of the future dynamics and the solution of an optimization problem online at each sampling time, updated by the new measurement [19]. The obtained control action is injected into the system until the next sampling time. In this brief, we will use the linearized model to predict the future error dynamics starting from $(t_k, x_e(t_k))$. In order to emphasize that the predicted error trajectory need not and will not be the same as the real one, we denote the predicted error trajectory as $(\bar{x}_e(\cdot), \bar{z}_e(\cdot))$, which is the solution of

$$\begin{aligned} \dot{\bar{x}}_e(\tau) &= A_k \bar{x}_e(\tau) + B_{1k} w(\tau) + B_{2k} u_e(\tau) \\ \bar{x}_e(t_k) &= x_e(t_k), \tau \geq t_k \end{aligned} \quad (10a)$$

$$\bar{z}_e(\tau) = C_k \bar{x}_e(\tau) + D_{1k} w(\tau) + D_{2k} u_e(\tau) \quad (10b)$$

with

$$\begin{pmatrix} A_k & B_{1k} & B_{2k} \\ C_k & D_{1k} & D_{2k} \end{pmatrix} = \begin{pmatrix} A(t_k) & B_1(t_k) & B_2(t_k) \\ C(t_k) & D_1(t_k) & D_2(t_k) \end{pmatrix} =: \Omega_k. \quad (11)$$

Knowing that a linearized model can only capture the local dynamics of the nonlinear system, we perform the linearization procedure at each sampling time t_k . Due to the time-varying property of the reference, this implies that the prediction at each sampling time will be based on different models and hence the optimization problem will be updated not only by the actual state (as usual) but also by the actual linearized model.

We observe that at each fixed sampling time t_k , (10) is a linear time-invariant (LTI) system, which simplifies significantly the issue. As suggested in [17], we solve the following matrix inequality optimization problem related to continuous constrained \mathcal{H}_∞ control to determine a state feedback gain:

$$\min_{\gamma^2, Q=Q^T > 0, Y} \gamma^2 \text{ subject to} \quad (12a)$$

$$\begin{pmatrix} A_k Q + Q A_k^T + B_{2k} Y + Y^T B_{2k}^T & * & * \\ B_{1k}^T & -\gamma^2 I & * \\ C_k Q + D_{2k} Y & D_{1k} & -I \end{pmatrix} < 0 \quad (12b)$$

$$\begin{pmatrix} r_c & x_e(t_k)^T \\ x_e(t_k) & Q \end{pmatrix} \geq 0 \quad (12c)$$

$$\begin{pmatrix} \frac{u_{jk, \max}^2}{r_c} & e_j^T Y \\ * & Q \end{pmatrix} \geq 0, j = 1, 2, \dots, m_2 \quad (12d)$$

$$\begin{pmatrix} p_0 - p_{k-1} + x_e(t_k)^T P_{k-1} x_e(t_k) & x_e(t_k)^T \\ x_e(t_k) & Q \end{pmatrix} \geq 0 \quad (12e)$$

where Q and Y are matrix variables with appropriate dimensions, $r_c > 0$ is a tuning parameter, e_j is the basis vector in \mathbb{R}^{m_2} and

$$u_{jk, \max} := \min_{t \in [t_k, t_{k+1})} \{u_{j, \max} - |u_{d,j}(t)|\}, \quad j = 1, 2, \dots, m_2. \quad (13)$$

Moreover, γ is the standard \mathcal{H}_∞ norm of the prediction model (10), that is defined in the infinite horizon and will be online minimized to achieve the best possible disturbance attenuation. We assume at this moment that this optimization problem is feasible, (we will discuss the feasibility issue in

Section III-C). With an (almost) optimal solution¹ at time t_k , denoted as (γ_k, Q_k, Y_k) , we determine the state feedback gain by $K_k = Y_k Q_k^{-1}$, and update (P_{k-1}, p_{k-1}) recursively as $P_k := Q_k^{-1}$ and

$$p_k := p_{k-1} - [x_e(t_k)^T P_{k-1} x_e(t_k) - x_e(t_k)^T P_k x_e(t_k)]. \quad (14)$$

The recursion is initialized by solving the optimization problem at the time t_0 without (12e), and by setting $P_0 = Q_0^{-1}$ and $p_0 = x_e(t_0)^T P_0 x_e(t_0)$. The closed-loop control is then computed by

$$u_e(t) = K_k x_e(t) \forall t \in [t_k, t_{k+1}), k \geq 0 \quad (15)$$

and furthermore for the given $x_d(\cdot)$ and $u_d(\cdot)$

$$u(t) = K_k(x(t) - x_d(t)) + u_d(t) \forall t \in [t_k, t_{k+1}), k \geq 0. \quad (16)$$

According to the principle of MPC, the feedback control (16) is applied to the system (3) until the next sampling time t_{k+1} . By defining $k := k+1$, we use actual values of the state and the reference to compute $x_e(t_k)$, Ω_k and $u_{jk, \max}$ by (6), (11), and (13), respectively. Then, the optimization problem (12) will be solved again.

Remark 3.1: In the optimization problem (12), (12a) is a standard LMI on (γ^2, Q, Y) for given Ω_k , which arises from the unconstrained \mathcal{H}_∞ control problem based on the prediction model (10). The inequality (12e) is the so-called dissipation constraint for ensuring the closed-loop system dissipative, which will be clear later. This form of constraint is first proposed in [20] and discussed in [17]. Since P_{k-1} and p_{k-1} are computed at the previous step, (12e) is also an LMI in Q for given $x_e(t_k)$. The inequalities (12c) and (12d) are introduced for the satisfaction of the control constraints, which will be clear next in the Proof of Theorem 1. They are LMIs in Q and Y for given $r_c, x_e(t_k)$ and $u_{jk, \max}$. Hence, if we have r_c fixed, (12) is an LMI optimization problem and can be effectively solved in the numerical manner. In this sense, the proposed approach is computationally tractable, whereas most existing robust MPC schemes could be viewed to be more conceptual rather than practical [19]. Moreover, the choice of r_c can be referred to [17].

Remark 3.2: The main feature of the proposed approach is to perform tracking control and achieve an \mathcal{H}_∞ performance in the simultaneous presence of control constraints and external disturbances. The designed controller is able to automatically relax the tracking performance level if necessary for avoiding actuator saturation in the case of unexpectedly large disturbances, and to enhance the performance level when the large disturbances vanish. This is also illustrated in Section IV.

Remark 3.3: The online optimization is a computationally expensive task and may preclude real-time implementations of the proposed algorithm for fast systems. This motivates our further efforts on reducing online computation time, for example the algorithm may be realized by field-programmable gate array (FPGA) or other embedding techniques.

¹With (almost) optimal solution we mean the solution of optimization problem is obtained through a numerical method with given parameters such as “relative accuracy for the optimal value”.

B. Closed-Loop Tracking Properties

Closed-loop tracking properties are discussed in the sequential consideration of three systems: the prediction model (10) with the feedback law $u_e = K_k x_e$, the linearized system (7) controlled by the moving horizon control (15), and, finally, the nonlinear system (3) controlled by the moving horizon control (16).

We assume that the optimization problem (12) at time t_k admits an (almost) optimal solution and denote it as (γ_k, Q_k, Y_k) . With $K_k = Y_k Q_k^{-1}$ and $P_k = Q_k^{-1}$, and by multiplying (12a) with $\text{diag}(P_k, I, I)$ on the left and right, we obtain an equivalence of (12b) as follows

$$\begin{pmatrix} P_k A_{cl,k} + A_{cl,k}^T P_k & * & * \\ B_{1k}^T P_k & -\gamma_k^2 I & * \\ C_{cl,k} & D_{1k} & -I \end{pmatrix} < 0 \quad (17)$$

where $A_{cl,k} = A_k + B_{2k} K_k$, $C_{cl,k} = C_k + D_{2k} K_k$. Taking the Schur complement, the previous matrix inequality is equivalent to

$$\begin{pmatrix} P_k A_{cl,k} + A_{cl,k}^T P_k + C_{cl,k}^T C_{cl,k} & * \\ B_{1k}^T P_k + D_{1k}^T C_{cl,k} & D_{1k}^T D_{1k} - \gamma_k^2 I \end{pmatrix} < 0. \quad (18)$$

Let us first consider the control of the systems (10) with the feedback law $u_e = K_k x_e$. By defining $V_k(x) := x^T P_k x$, it is then standard to show that the feasibility of (18) leads to the integral dissipation inequality

$$V_k(\bar{x}_e(\tau)) + \int_{t_k}^{\tau} \|\bar{z}_e(s)\|^2 - \gamma_k^2 \|w(s)\|^2 ds \leq V_k(\bar{x}_e(t_k)). \quad (19)$$

Second, we consider the linearized system (7) controlled by (15). Since $\bar{x}_e(t_k) = x_e(t_k)$, by the *continuity of the system dynamics* and the assumption of *sufficiently small sampling times*, we conclude from (19) the following inequality for all $t \in [t_k, t_{k+1})$:

$$V_k(x_e(t)) + \int_{t_k}^t \|z_e(s)\|^2 - \gamma_k^2 \|w(s)\|^2 ds \leq V_k(x_e(t_k)). \quad (20)$$

We stress that (20) is only valid for the *sufficiently small* time interval $[t_k, t_{k+1})$ and does not imply the dissipation of the closed-loop system (7) with (15). But, it serves as a starting point for the purpose, as shown in the following.

By the moving horizon strategy of MPC, the optimization problem is solved repeatedly at each sampling time. And under the existence assumption, this implies that (20) with the pair (V_k, γ_k) is valid for $k = 0, 1, 2, \dots$, i.e.,

$$\begin{aligned} x_e(t_1)^T P_0 x_e(t_1) - x_e(t_0)^T P_0 x_e(t_0) \\ \leq - \int_{t_0}^{t_1} \|z_e(s)\|^2 + \gamma_0^2 \|w(s)\|^2 ds \end{aligned} \quad (21a)$$

$$\begin{aligned} x_e(t_2)^T P_1 x_e(t_2) - x_e(t_1)^T P_1 x_e(t_1) \\ \leq - \int_{t_1}^{t_2} \|z_e(s)\|^2 + \gamma_1^2 \|w(s)\|^2 ds \end{aligned} \quad (21b)$$

$$\begin{aligned} & \vdots \\ & x_e(t)^T P_k x_e(t) - x_e(t_k)^T P_k x_e(t_k) \\ & \leq - \int_{t_k}^t \|z_e(s)\|^2 + \gamma_k^2 \|w(s)\|^2 ds \\ & \forall t \in [t_k, t_{k+1}). \end{aligned} \quad (21c)$$

Hence, simple addition operations lead to that the closed-loop system (7) with (15) obeys

$$\begin{aligned} & \int_{t_0}^t \|z_e(s)\|^2 - \gamma(s)^2 \|w(s)\|^2 ds \\ & \leq V_0(x_e(t_0)) - V_k(x_e(t)) \\ & \quad - \sum_{i=1}^k [x_e(t_i)^T P_{i-1} x_e(t_i) - x_e(t_i)^T P_i x_e(t_i)] \end{aligned} \quad (22)$$

for all $t \in [t_k, t_{k+1})$ and all $k > 0$, where $\gamma(\cdot)$ is piece-wise constant and defined by $\gamma(t) := \gamma_i$ for all $t \in [t_i, t_{i+1})$, $i \geq 0$. On the other hand, the feasibility of the dissipation constraint (12e) enforces [17]

$$\sum_{i=1}^k [x_e(t_i)^T P_{i-1} x_e(t_i) - x_e(t_i)^T P_i x_e(t_i)] \geq 0. \quad (23)$$

Combining it with (22) leads to

$$V_k(x_e(t)) - V_0(x_e(t_0)) \leq \int_{t_0}^t \gamma(s)^2 \|w(s)\|^2 - \|z_e(s)\|^2 ds. \quad (24)$$

We now define a storage function as $V(t, x) := x^T P_k x$, $t \in [t_k, t_{k+1})$, $k \geq 0$ and conclude that the closed-loop system (7) with (15) satisfies

$$V(t, x_e(t)) - V(t_0, x_e(t_0)) \leq \int_{t_0}^t \gamma(s)^2 \|w(s)\|^2 - \|z_e(s)\|^2 ds \quad (25)$$

for all $t \geq t_0$. Clearly, if the sequence of P_k is norm-bounded, then $\alpha_1 \|x\|^2 \leq V(t, x) \leq \alpha_2 \|x\|^2$ for some $\alpha_1 > 0$ and $\alpha_2 > 0$.

We are now ready to state the following result for the linearized system (7) controlled with (15).

Theorem 1: Suppose the following:

- solution of the system (7) is unique and sufficiently smooth;
- amplitude of the disturbances is bounded;
- sampling time is sufficiently small;
- optimization problem (12) admits an almost optimal and norm-bounded solution at each sampling time.

Then, the closed-loop system (7) with the moving horizon control (15) has the following properties:

- (i) the time-domain constraints (9) are satisfied;
- (ii) it is dissipative;
- (iii) it is asymptotically stable for vanishing disturbances, if (7) is uniformly zero-observable.

Proof: By taking the Schur complement, the feasibility of (12c) with $Q = Q_k$ implies that the actual error state $x_e(t_k)$ is in an ellipsoid defined by $\mathcal{E}(P_k, r_c) := \{x \in \mathbb{R}^n : x^T P_k x \leq r_c\}$.

If the amplitude of the disturbances is bounded, i.e., $\|w(t)\| < \infty, \forall t \geq t_0$, then we have $\lim_{t \rightarrow t_k} \int_{t_k}^t \gamma_k^2 \|w(s)\|^2 ds \rightarrow 0$ for bounded γ_k . It follows then from (20) that

$$\lim_{t \rightarrow t_k} \left\{ V_k(x_e(t)) + \int_{t_k}^t \|z_e(s)\|^2 ds \right\} \leq V_k(x_e(t_k)) \quad (26)$$

which implies that for a sufficiently small sampling time, the error state trajectory on $[t_k, t_{k+1})$ starting from $x_e(t_k) \in \mathcal{E}(P_k, r_c)$ remains in the same ellipsoid. Hence, we can infer that

$$\begin{aligned} \max_{t \in [t_k, t_{k+1})} |u_{e,j}(t)|^2 &= \max_{t \in [t_k, t_{k+1})} |e_j^T Y_k Q_k^{-1} x_e(t)|^2 \\ &\leq \max_{x \in \mathcal{E}(P_k, r_c)} |e_j^T Y_k Q_k^{-1} x|^2 \\ &\leq r_c \left\| e_j^T Y_k Q_k^{-\frac{1}{2}} \right\|_2^2. \end{aligned} \quad (27)$$

Due to the feasibility of (12d) with $Q = Q_k$ and $Y = Y_k$, the previous inequality becomes $\max_{t \in [t_k, t_{k+1})} |u_{e,j}(t)| \leq u_{jk, \max}$, which is valid for all $t \geq t_0$ and all $j = 1, 2, \dots, m_2$. By (13), we arrive at the satisfaction of the control constraints (9), as required in (i).

Property (ii) is a direct result from (25). If furthermore the disturbances are vanishing, then for bounded $\gamma(t)$, we have $\gamma(t)\|w(t)\| \rightarrow 0$ as $t \rightarrow \infty$. We can take the limit $t \rightarrow \infty$ for (25) to arrive at

$$\int_{t_0}^{\infty} \|z_e(t)\|^2 dt \leq V(t_0, x_e(t_0)) + \int_{t_0}^{\infty} \gamma(t)^2 \|w(t)\|^2 dt < \infty. \quad (28)$$

This indicates $z_e(t) \rightarrow 0$ as $t \rightarrow \infty$ independent of t_0 , and hence the asymptotic stability property by the assumption of the uniform zero-observability [21], as required in (iii). \square

Remark 3.4: In the previous section, we use the condition of sufficiently small sampling times to obtain (20) from (19). This condition is indeed difficult to verify. More may be rigorously discussed in the framework of sampled-data control (e.g., [22]), but that is out of the scope of this brief. In the case of non-small-enough sampling times, from (20) we still have $V_k(x_e(t)) \leq V_k(x_e(t_k)), \forall t \in [t_k, t_{k+1})$, if the disturbance amplitude satisfies $\int_{t_k}^{t_{k+1}} \|w(s)\|^2 ds \leq (\int_{t_k}^{t_{k+1}} \|z_e(s)\|^2 ds) / (\gamma_k^2)$. Then, the property (i) is still valid.

Finally, we focus on the tracking error of the nonlinear system (3) controlled by the moving horizon control (16). We notice that (16) satisfies $u(t) = u_d(t)$ if there is no tracking error, i.e., $x(t) = x_d(t)$. Since (z_d, x_d, u_d) satisfies (5), the point (0,0) is then an equilibrium of the nonlinear error system. Therefore, we can recall the following lemma to show the \mathcal{L}_2 disturbance attenuation for the tracking error.

Lemma 1: [23] Given $\gamma > 0$. Suppose that the linearized system of a nonlinear system at the equilibrium is asymptotically stable and admits an \mathcal{L}_2 gain less than γ . Then, there exists a neighborhood of the equilibrium such that the nonlinear system admits locally an \mathcal{L}_2 gain less than γ .

Theorem 2: Suppose that the assumptions in Theorem 1 are satisfied and the linearized system (7) is uniformly zero-observable. Then, for vanishing disturbances, the nonlinear system (3)

controlled with the moving horizon control (16) achieves the following:

- (i) control constraints (4) are satisfied;
- (ii) tracking error is locally asymptotically stable;
- (iii) disturbances are attenuated in the sense of the local \mathcal{L}_2 gain from the disturbance w to the tracking output error z_e less than $\bar{\gamma}$, where $\bar{\gamma}$ is defined by $\bar{\gamma} := \max_{t \geq t_0} \gamma(t)$.

Proof: It follows from the result (i) in Theorem 1 that $|u_{e,j}(t)| \leq u_{jk, \max}$. By (13), we have then

$$|u_j(t)| \leq |u_{e,j}(t)| + |u_{d,j}(t)| \leq u_{j, \max} \quad (29)$$

for all $t \geq t_0$ and $j = 1, 2, \dots, m_2$, as required in (i).

We now consider the two closed-loop systems with the moving horizon control: the nonlinear system (3) controlled with (16), denoted as System A, and the linearized system (7) with (15), denoted as System B. By (15) and (16), we notice that the linearization of System A about the given reference is just System B. Hence, the local stability property of the tracking error follows from the result (iii) of Theorem 1, due to the zero-detectability (e.g., [21]). By defining $\bar{\gamma} := \max_{t \geq t_0} \gamma(t)$, then, (25) becomes

$$\int_{t_0}^{\infty} \|z_e(t)\|^2 dt \leq x_e(t_0)^T P_0 x_e(t_0) + \int_{t_0}^{\infty} \bar{\gamma}^2 \|w(t)\|^2 dt \quad (30)$$

for System B. Hence, we can apply Lemma 1 to conclude that there exists a neighborhood along the reference such that the tracking error admits locally an \mathcal{L}_2 gain less than $\bar{\gamma}$, as required in (iii). \square

C. Improved Algorithm

It is shown in [17] that a prior feasibility of the control scheme can be guaranteed if restrictive hypotheses are imposed on the external disturbances. In the previous discussion, we do not mention such hypotheses, since it is difficult, if not impossible, to obtain a prior disturbance information. In order to avoid infeasibility of (12), which may occur especially when unexpectedly large disturbances are encountered, [24] suggests an improved algorithm by the use of Lagrange duality. Hence, we now modify the online solved optimization problem as follows:

$$\begin{aligned} \min_{r, \gamma^2, Q=Q^T > 0, Y} \quad & q_1 r \\ & + q_2 \gamma^2 \text{ subject to (12b), (12d), (12e), and} \end{aligned} \quad (31a)$$

$$\begin{pmatrix} r & x_e(t_k)^T \\ x_e(t_k) & Q \end{pmatrix} \geq 0, r \leq r_c(1 + \epsilon) \quad (31b)$$

where q_1 and q_2 are weights, $\epsilon \geq 0$ is introduced to avoid infeasibility. The corresponding algorithm is given as follows.

Algorithm 1:

- S1 Initialization. Set r_c .
- S2 At time $t_0(k = 0)$, get $(x(t_0), x_d(t_0), u_d(t_0))$ and compute $x_e(t_0)$ by (6), Ω_0 by (11) and $u_{j0, \max}$ by (13). Set $\epsilon = 0$, solve the LMI optimization problem (31) without (12e) to obtain $(r_0, \gamma_0, Q_0, Y_0)$. Compute $K_0 = Y_0 Q_0^{-1}$, $P_0 = Q_0^{-1}$, $p_0 = x_e(t_0) P_0 x_e(t_0)$ and go to S5.

- S3 At time $t_k > t_0 (k \geq 1)$, get $(x(t_k), x_d(t_k), u_d(t_k))$ and compute $x_e(t_k)$ by (6), Ω_k by (11) and $u_{jk, \max}$ by (13). Set $\epsilon = 0$, solve the optimization problem (31) to obtain $(r_k, \gamma_k, Q_k, Y_k)$. If not feasible, solve it with increasing $\epsilon > 0$. Compute $K_k = Y_k Q_k^{-1}$.
- S4 Prepare for the next computation: Compute $P_k = Q_k^{-1}$ and compute p_k according to (14).
- S5 Compute the closed-loop control by (16). Replace k by $k + 1$ and go to S3.

In Algorithm 1, we first shape the ellipsoid $\mathcal{E}(P, r)$ through on-line optimization to contain the actual state $x_e(t_k)$. If successful, then, (12d) and $r \leq r_c$ guarantee the satisfaction of the control constraint. If not successful, the ellipsoid is relaxed by increasing $\epsilon > 0$. Then, we can compute the feedback gain K_k and check the satisfaction of the control constraint by

$$|e_j^T K_k (x(t_k) - x_d(t_k)) + u_{d,j}(t_k)| \leq u_{j, \max}, \quad j = 1, 2, \dots, m_2. \quad (32)$$

This way, the conservatism involving in the ellipsoid evaluation of time-domain constraints is some extent reduced. This is clarified in [24] and clearly seen in Section IV.

The properties of the closed-loop system are then given in the following theorem.

Theorem 3: Suppose the following:

- first three assumptions in Theorem 1 are satisfied;
- linearized system (7) is uniformly zero-observable;
- at each sampling time t_k , a feedback gain K_k can be determined by Algorithm 1.

Then, the control constraints in (4) are respected, if the obtained K_k satisfies (32). Moreover, the nonlinear system (3) controlled with (16) achieves the properties (ii) and (iii) in Theorem 2.

Proof: The satisfaction of the control constraint is obvious and the rest of the proof is the same as that of Theorem 2. \square

IV. SIMULATION RESULTS

In this section, we apply our moving horizon \mathcal{H}_∞ control approach to the tracking problem of the constrained WMR described in Section II. Hence, we use in the following the WMR notation and let $\xi := [x, y, \phi, v, \omega]^T$ and $u := [\tau_1, \tau_2]^T$ for a condensed presentation. Moreover, the subscripts “d” and “e” are denoted as reference and tracking error, respectively. As an example we take the LABMATE robot described in [25]. One can find a more detailed description of this robot in [25], whereas we only list its physical parameters as follows: $m = 80$ kg, $I = 2$ kg·m², $b = 0.075$ m, $l = 0.325$ m. In addition, due to actuator saturation, control inputs are assumed to be constrained as $|\tau_1(t)| \leq 4$ N·m, $|\tau_2(t)| \leq 4$ N·m, $t \geq 0$. We now report simulation results of tracking an eight-shaped trajectory defined by $x_d(t) = a_1 \sin(t/a_3)$, $y_d(t) = a_2 \sin(t/2a_3)$, $t \geq 0$. As mentioned in Section II, the reference trajectory (ξ_d, u_d) has to be consistent with the unperturbed WMR model and feasible for the non-holonomic constraint. To ensure this, we apply the differential flatness technique [26] and choose (x, y) as the flatness outputs. Then, all the states and inputs can be represented as

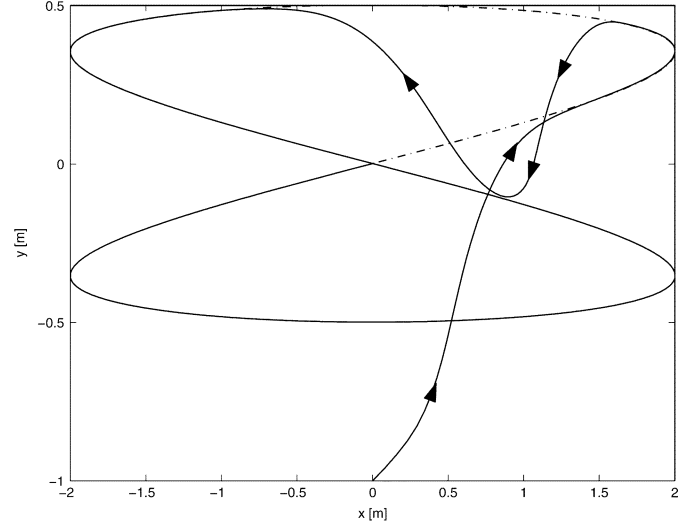


Fig. 3. Desired eight-shaped reference trajectory (— · —) and the real tracking trajectory (—).

the functions of (x, y) and their time derivatives. The obtained reference input u_d is as follows:

$$u_d = \begin{bmatrix} \frac{s_1 + s_2}{2}, & \frac{s_1 - s_2}{2} \end{bmatrix} \quad (33)$$

where

$$s_1 = \frac{\dot{x}_d \ddot{x}_d + \dot{y}_d \ddot{y}_d}{\beta_1 \sqrt{\dot{x}_d^2 + \dot{y}_d^2}},$$

$$s_2 = \frac{\dot{x}_d \ddot{y}_d - \ddot{x}_d \dot{y}_d}{\beta_2 (\dot{x}_d^2 + \dot{y}_d^2)} - \frac{2(\dot{x}_d \ddot{y}_d - \ddot{x}_d \dot{y}_d)(\dot{x}_d \ddot{x}_d + \dot{y}_d \ddot{y}_d)}{\beta_2 (\dot{x}_d^2 + \dot{y}_d^2)^2}.$$

Moreover, as the function of (a_1, a_2, a_3, t) , u_d has to satisfy the control constraint (2) at any time $t \geq 0$. Finding the set of all combinations of (a_1, a_2, a_3) , for which the corresponding eight-shaped trajectory respects (2), is out of the scope of this brief, we just choose $a_1 = 2$, $a_2 = 0.5$, and $a_3 = 7$ in the simulation such that u_d remains within their bounds. The specified eight-shaped trajectory is shown in Fig. 3 as dashed-dotted line, where $x_d(0) = 0$ and $y_d(0) = 0$.

About the given reference trajectory, the linearized system matrices are computed by (8) as follows:

$$A(t) = \begin{pmatrix} 0 & 0 & -v_d(t) \sin \phi_d(t) & \cos \phi_d(t) & 0 \\ 0 & 0 & v_d(t) \cos \phi_d(t) & \sin \phi_d(t) & 0 \\ 0 & 0 & 0 & 0 & 1 \\ 0 & 0 & 0 & 0 & 0 \\ 0 & 0 & 0 & 0 & 0 \end{pmatrix}$$

$$B_1(t) = \begin{pmatrix} 0 & 0 \\ 0 & 0 \\ 0 & 0 \\ \beta_3 & 0 \\ 0 & \beta_4 \end{pmatrix}$$

$$B_2(t) = \begin{pmatrix} 0 & 0 \\ 0 & 0 \\ 0 & 0 \\ \beta_1 & \beta_1 \\ \beta_2 & -\beta_2 \end{pmatrix}.$$

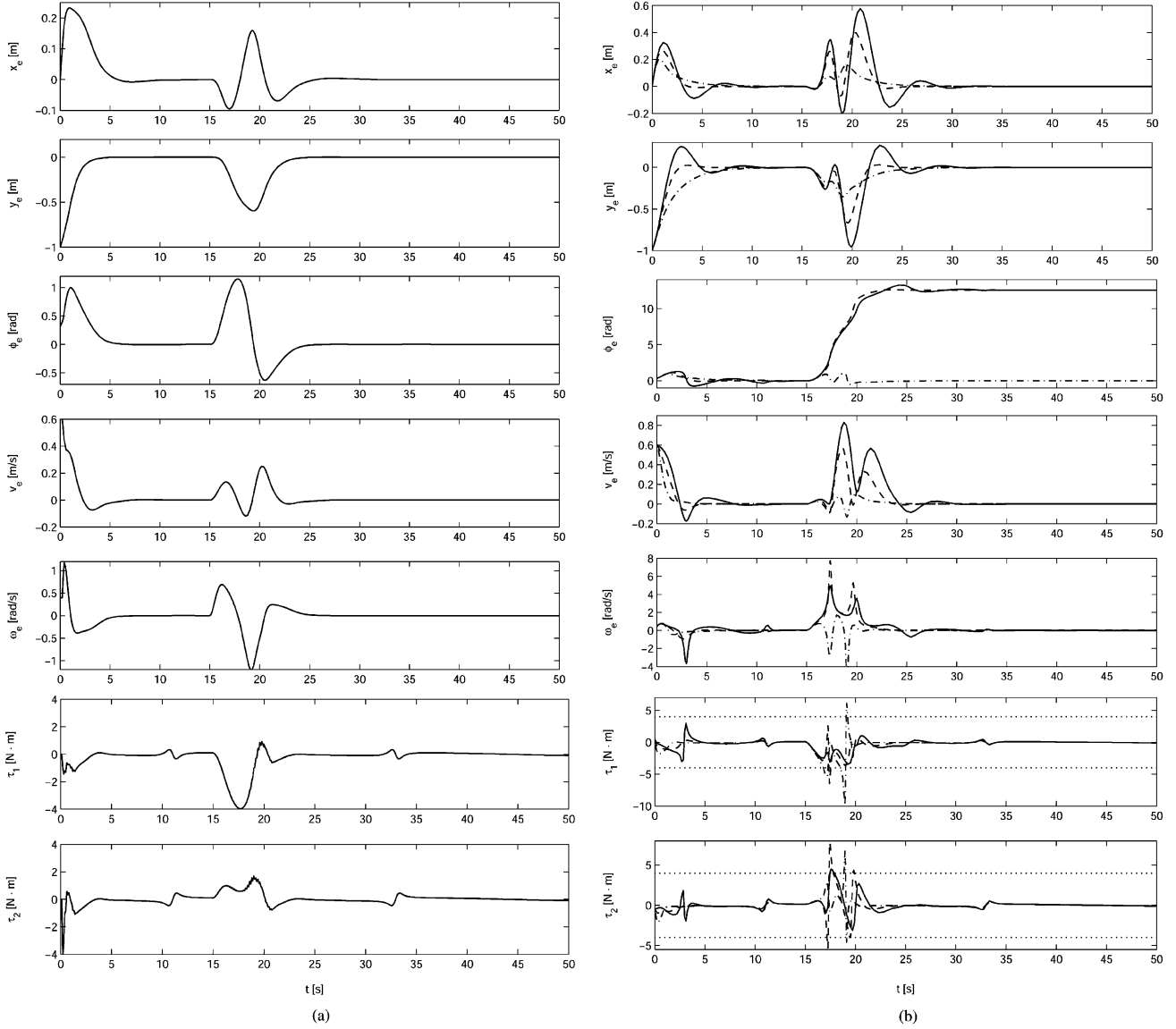


Fig. 4. Tracking errors x_e [m], y_e [m], ϕ_e [rad], v_e [m/s], ω_e [rad/s] and control inputs τ_1 [N · m], τ_2 [N · m]. (a) Moving horizon \mathcal{H}_∞ tracking controller. (b) Dynamic feedback linearization tracking controller.

The matrices in the performance output (7b) are chosen as $C(t) = \text{diag}\{2, 2, 0.7, 0.5, 0.5\}$, and $D_1(t) = D_2(t) = 0_{5 \times 2}$. The tuning parameters in (31) are chosen as $r_c = 1$, $q_1 = 2$, $q_2 = 1$. The simulation is performed by Algorithm 1 with a sampling time of $T = 0.2$ s, which is chosen according to Remark 3.4 and by trial and error. The results are plotted in Figs. 4(a) and 5, where the robot starts with the initial error of $\xi_e(0) = [0, -1, \pi/10, 0.6, 0.4]^T$ and suffers two disturbances of $w_1 = 32.04 \sin(2\pi t/10)$ [N] and $w_2 = 18.50 \sin(2\pi t/10)$ [N · m] during $15 \text{ s} \leq t \leq 20 \text{ s}$. For a total simulation of 50 s, the elapsed CPU time is about 93 s in a system with 2.4 GHz X86 CPU and 512 M RAM, where the controller calls `mincx` for solving the LMI optimization problem with given numerical parameters (relative accuracy = 0.01, etc.). The heavy online computation burden arises partially from the M-files management.

The trajectory is shown in Fig. 3 as arrowed solid line. Although there are large initial errors, the robot converges to the reference trajectory. Then, it goes away from it due to the disturbance and converges again later. The plots in Fig. 4 show also that the controlled WMR tracks the given reference trajectory well in spite of the large initial errors and external disturbances, while the control actions remain within their bounds. From the time profile of γ plotted in the bottom of Fig. 5, we see that the moving horizon \mathcal{H}_∞ tracking controller relaxes automatically the performance level if necessary for the satisfaction of control constraints. In Fig. 5, we also plot the time profile of $\xi_e^T(t) P_k \xi_e(t) / r_c$. A clear violation of $\xi_e^T(t) P_k \xi_e(t) \leq r_c$ can be seen at the beginning and during the effect of disturbances, which implies that the optimization problem (12) was infeasible. This verifies the improvement of Algorithm 1 in avoiding infeasibility.

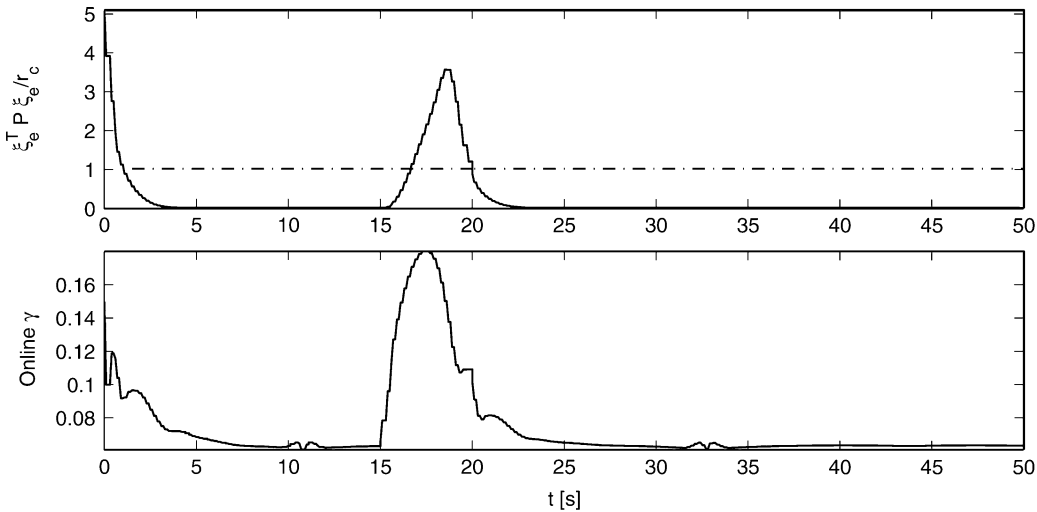


Fig. 5. Profiles of $\xi_e^T(t)P_k\xi_e(t)/r_c$ and $\gamma(t)$.

As comparison, we design a tracking controller by dynamic feedback linearization [27]. Without considering disturbances and control constraints, the following dynamic compensator:

$$\begin{cases} \dot{\eta} &= \frac{v_1 \cos \phi + v_2 \sin \phi + v \omega^2}{\beta_1} \\ \tau_1 + \tau_2 &= \eta \\ \tau_1 - \tau_2 &= \frac{v_2 \cos \phi - v_1 \sin \phi - 2\beta_1 \xi \omega}{v\beta_2} \end{cases} \quad (34)$$

renders the original nonlinear system linearized as $\ddot{x} = v_1$ and $\ddot{y} = v_2$. In order to asymptotically track the desired trajectory, v_1 and v_2 can be designed as

$$\begin{cases} v_1 &= \ddot{x}_d + k_{a1}(\ddot{x}_d - \ddot{x}) + k_{p1}(\dot{x}_d - \dot{x}) + k_{d1}(x_d - x) \\ v_2 &= \ddot{y}_d + k_{a2}(\ddot{y}_d - \ddot{y}) + k_{p2}(\dot{y}_d - \dot{y}) + k_{d2}(y_d - y) \end{cases} \quad (35)$$

with gains chosen as $k_{ai} > 0, k_{pi} > 0, k_{di} > 0$, for $i = 1, 2$. The results with three selected sets of gains (A: $k_{ai} = k_{di} = 4, k_{pi} = 6(-)$, B: $k_{ai} = k_{di} = 4, k_{pi} = 10(- \cdot -)$, C: $k_{ai} = k_{di} = 4, k_{pi} = 4(-)$, $i = 1, 2$) are plotted in Fig. 4(b). It is clear that the control inputs with set A and set B go beyond the bounds due to the disturbances. The control effort could be made acceptable by a proper choice of the gains, at the cost of the performance (since high-gain controllers are required for good performance). This is illustrated by the results with the gain set C in Fig. 4(b) as solid lines. The moving horizon \mathcal{H}_∞ tracking controller can manage automatically between achieving good tracking performance and satisfying control constraints (see Figs. 4(a) and 5).

V. CONCLUSION

The tracking problem of non-holonomic WMRs in the presence of actuator saturation and external disturbances is addressed, by the use of moving horizon control strategy. To predict the future error dynamics at each sampling time, the nonlinear dynamic WMR is linearized online along the reference trajectory. This simplification renders the constrained disturbance attenuation problem tractable in the use of LMI optimization. Then, a moving horizon \mathcal{H}_∞ tracking control

scheme and a computationally tractable algorithm are proposed. Through online optimization, the tracking controller is able to automatically relax the performance level if necessary to satisfy control constraints in the case for example of unexpectedly large disturbances, and to enhance the level when the large disturbances vanish. This is confirmed by simulation results of tracking an eight-shaped trajectory in the presence of both control constraints and external disturbances. Closed-loop tracking properties inclusive of \mathcal{L}_2 disturbance attenuation are discussed in the framework of dissipation theory.

REFERENCES

- [1] C. Samson and K. Ait-Abderrahim, "Feedback control a nonholonomic wheeled cart in Cartesian space," in *Proc. IEEE Int. Conf. Robot. Autom.*, Sacramento, CA, 1991, pp. 1136–1141.
- [2] A. M. Bloch and S. Drakunov, "Tracking in nonholonomic dynamic system via sliding modes," in *Proc. 34th IEEE Conf. Decision Control*, New Orleans, LA, 1995, pp. 2103–2106.
- [3] Z. P. Jiang and H. Nijmeijer, "A recursive technique for tracking control of nonholonomic systems in chained form," *IEEE Trans. Autom. Control*, vol. 44, no. 2, pp. 265–279, Feb. 1999.
- [4] J.-M. Yang and J.-H. Kim, "Sliding mode control for trajectory tracking of nonholonomic wheeled robots," *IEEE Trans. Robot. Autom.*, vol. 15, no. 3, pp. 578–587, Jun. 1999.
- [5] D. Chwa, "Sliding-mode tracking control of nonholonomic wheeled mobile robots in polar coordinates," *IEEE Trans. Control Syst. Technol.*, vol. 12, no. 4, pp. 637–614, July 2004.
- [6] B. d'Andrea Novel, G. Bastin, and C. G., "Control of nonholonomic wheeled mobile robots by state feedback linearization," *Int. J. Robot. Res.*, vol. 14, no. 6, pp. 543–559, 1995.
- [7] G. Oriolo, A. De Luca, and M. Vendittelli, "WMR control via dynamic feedback linearization: Design, implementation, and experimental validation," *IEEE Trans. Control Syst. Technol.*, vol. 10, no. 6, pp. 835–852, Nov. 2002.
- [8] Z. P. Jiang, E. Lefeber, and H. Nijmeijer, "Saturated stabilization and tracking of a nonholonomic mobile robot," *Syst. Control Lett.*, vol. 42, pp. 327–332, 2001.
- [9] T. C. Lee, K. T. Song, C. H. Lee, and T. C. C., "Tracking control of unicycle-modeled mobile robots using a saturation feedback controller," *IEEE Trans. Control Syst. Technol.*, vol. 9, no. 2, pp. 305–318, Mar. 2001.
- [10] W. Ren, J.-S. Sun, R. W. Beard, and T. W. McLain, "Nonlinear tracking control for nonholonomic mobile robots with input constraints: An experimental study," in *Proc. Amer. Control Conf.*, Jun. 2005, pp. 4923–4928.

- [11] H. A. van Essen and H. Nijmeijer, "Nonlinear model predictive control for constrained mobile robots," presented at the Eur. Control Conf., Porto, Portugal, 2001.
- [12] F. A. C. C. Fontes and L. Magni, "Min-max model predictive control of nonlinear systems using discontinuous feedbacks," *IEEE Trans. Automat. Control*, vol. 48, no. 10, pp. 1750–1755, Oct. 2003.
- [13] F. Kühne, W. F. Lages, and J. M. Gomes da Silva Jr., "Model predictive control of a mobile robot using linearization," in *Proc. IEEE Conf. Mechatron. Robot.*, Aachen, Germany, 2004, pp. 525–530.
- [14] D.-B. Gu and H.-S. Hu, "Receding horizon tracking control of wheeled mobile robots," *IEEE Trans. Control Syst. Technol.*, vol. 14, no. 4, pp. 743–749, Jul. 2006.
- [15] Z. P. Wang, S. S. Ge, and T. H. Lee, "Robust motion/force control of uncertain holonomic/nonholonomic mechanical systems," *IEEE/ASME Trans. Mechatronics*, vol. 9, no. 1, pp. 118–123, Feb. 2004.
- [16] P. Coelho and U. Nunes, "Path-following control of mobile robots in presence of uncertainties," *IEEE Trans. Robot.*, vol. 21, no. 2, pp. 1445–1450, Mar. 2005.
- [17] H. Chen and C. W. Scherer, "Moving horizon H_∞ control with performance adaptation for constrained linear systems," *Automatica*, vol. 42, no. 6, pp. 1033–1040, 2006.
- [18] M. J. van Nieuwstadt and R. M. Murray, "Real-time trajectory generation for differentially flat systems," *Int. J. Robust Nonlinear Control*, vol. 8, no. 11, pp. 995–1020, 1998.
- [19] D. Q. Mayne, J. B. Rawlings, C. V. Rao, and P. O. M. Scokaert, "Constrained model predictive control: Stability and optimality," *Automatica*, vol. 36, no. 6, pp. 789–814, 2000.
- [20] C. W. Scherer, H. Chen, and F. Allgöwer, "Disturbance attenuation with actuator constraints by hybrid state-feedback control," in *Proc. 41th IEEE Conf. Decision Control*, Las Vegas, NV, Dec. 2002, pp. 4134–4139.
- [21] H. Khalil, *Nonlinear Systems*. New York: Macmillan, 1992.
- [22] T. Chen and B. Francis, *E Optimal Sampled-Data Control Systems*. New York: Springer-Verlag, 1995.
- [23] A. van der Schaft, *L_2 -Gain and Passivity Techniques in Nonlinear Control*. London, U.K.: Springer-Verlag, 2000.
- [24] H. Chen, X.-Q. Gao, and H. Wang, "An improved moving horizon H_∞ control scheme through L agrange duality," *Int. J. Control*, vol. 79, no. 3, pp. 239–248, 2006.
- [25] M. L. Corradini and G. Orlando, "Control of mobile robots with uncertainties in the dynamical model: A discrete time sliding mode approach with experimental results," *Control Eng. Practice*, vol. 10, no. 1, pp. 23–34, 2002.
- [26] M. Fliess, J. L'evine, P. Martin, and P. Rouchon, "Design of trajectory stabilizing feedback for driftless flat systems," in *Proc. 3rd Euro. Control Conf. ECC*, Rome, Italy, 1995, pp. 1882–1887.
- [27] A. Isidori, *Nonlinear Control Systems*, 3rd ed. Berlin, Germany: Springer-Verlag, 1995.